Int. J. Heat Mass Transfer. Vol. 27, No. 5, pp. 723–737, 1984
Printed in Great Britain

0017–9310/84 $3.00 + 0.00
Pergamon Press Ltd.

FLOW REGIME TRANSITION CRITERIA FOR UPWARD TWO-PHASE FLOW IN VERTICAL TUBES*

KAICHIRO MISHIMA
Research Reactor Institute, Kyoto University,
Kumatori, Osaka 590-04, Japan

and

MAMORU ISHII
Reactor Analysis and Safety Division, Argonne National Laboratory,
Argonne, IL 60439, U.S.A.

(*Received* 13 *January* 1983 *and in revised form* 29 *August* 1983)

Abstract – Traditional two-phase flow-regime criteria based on the gas and liquid superficial velocities may not be suitable to the analyses of rapid transient or entrance flows by the two-fluid model. Under these conditions, it is postulated that direct geometrical parameters such as the void fraction are conceptually simpler and therefore more reliable parameters to be used in flow-regime criteria than the traditional parameters. From this point of view, new flow-regime criteria for upward gas–liquid flow in vertical tubes have been developed considering the mechanisms of flow-regime transitions. These new criteria can be compared to existing criteria and experimental data under steady-state and fully developed flow conditions by using relative velocity correlations. The criteria showed reasonable agreements with the existing data for atmospheric air–water flows. Further comparisons with data for steam–water in round tubes and a rectangular channel at relatively high system pressures have been made. The results confirmed that the present flow-regime transition criteria could be applied over wide ranges of parameters as well as to boiling flow.

NOMENCLATURE

A	flow area of a tube
a	non-dimensional group defined by equation (20)
b	dimensional group defined by equation (21)
C_f	a constant
C_0	distribution parameter
D	hydraulic diameter
f	wall friction factor
G	mass velocity of two-phase mixture
g	gravity
h	distance from the nose of a slug bubble
j	superficial velocity of two-phase mixture
j_k	superficial velocity of k phase
L_b	mean slug-bubble length
l	gap between two bubbles
m	a constant
$N_{\mu f}$	viscosity number
p	pressure
r_b	mean bubble radius
v_{fsb}	terminal film velocity in the slug-bubble section
v_{gs}	gas velocity in the slug bubble
X	parameter defined by equation (12)
x_e	thermal equilibrium quality
y	dimensional group defined by equation (25).

Greek symbols

α	void fraction
α_m	mean void fraction
α_{sb}	void fraction corresponding to the terminal film velocity v_{fsb}
$\Delta\rho$	absolute value of density difference
μ_f	viscosity of liquid
ν_f	kinematic viscosity of liquid
ρ_k	density of k phase
σ	surface tension.

Subscripts

b	bubble
e	thermal equilibrium
f	liquid phase or friction
g	gas phase
m	mean
sb	tail-end of the slug bubble
s	slug bubble.

1. INTRODUCTION

IN ANALYZING two-phase flow transients such as in nuclear reactors under various accident conditions, a two-fluid model is very important because of its detailed description of thermohydraulic transients and phase interactions. The main difficulties in modeling arise from the existence of interfaces between phases and discontinuities associated with them. The internal structures of two-phase flow are classified by the flow regimes or flow patterns. Various transfer mechanisms

* All correspondence related to this paper should be addressed to M. Ishii, ANL.

between two-phase mixture and the wall, as well as between two phases, depend on the flow regimes. This leads to the use of regime dependent correlations together with two-phase flow-regime criteria. From this point of view, many works have been undertaken to predict flow regimes [1–12].

Traditionally, flow regimes are identified from a flow-regime map obtained from experimental observations. Many flow-regime maps have been proposed using dimensional coordinates based on the liquid and gas superficial velocities [1–4]. Other investigators have attempted to correlate the transition boundaries by non-dimensional groups [5–9]. There have also been theoretical works [10–12] to predict flow regimes. These conventional flow-regime maps are based primarily on the liquid and gas superficial velocities or the total mass flux and quality. The flow regimes are the classifications of the geometrical structures of flow. Therefore, it is postulated that the flow structures should depend directly on the geometrical parameter such as the void fraction and interfacial area. Under steady state fully developed conditions, it may be assumed that there exists a unique relation between the void fraction and the superficial velocities [2, 3, 14]. Therefore it can be said that these traditional approaches may be suitable for slow transients and near fully developed conditions, where a mixture model such as the drift-flux model is sufficient. The discrepancies between these two different approaches can be significant near flow reversal conditions or under rapid transient conditions, though these differences have not yet been clearly demonstrated by specially designed experiments.

However, in view of the practical applications of the two-fluid model to transient analysis, the flow-regime criteria based on the superficial velocities of liquid and gas may not be consistent with the two-fluid model formulation. This can be explained as follows. From the basic definitions of variables, the void fraction can be uniquely determined from the superficial velocities j_g and j_f and the relative velocity [14]. In the two-fluid model, the relative velocity is an unknown to be solved from the field equations. Therefore, the void fraction, which is the most important geometrical parameter, cannot be determined uniquely from superficial velocities j_g and j_f. Consequently, a flow-regime map based on j_g and j_f alone may be unsuitable to the two-fluid model formulation. This difficulty does not arise in the drift-flux model because the constitutive relation for the relative velocity can be used to determine the void fraction. However, for a two-fluid model, a direct geometrical parameter such as the void fraction may be more suitable to use in flow regime criteria than the traditional parameters.

In view of these, new flow-regime criteria for upward gas–liquid flow in vertical tubes have been developed in this study. Four basic flow regimes designated by Hewitt and Hall-Taylor [13] as bubbly flow, slug flow, churn flow and annular flow, have been analyzed. These new criteria can be compared to existing flow-regime maps under steady-state conditions by using relative velocity correlations obtained previously [14].

2. CRITERIA FOR FLOW-REGIME TRANSITIONS

2.1. *Bubbly flow to slug flow transition*

As studied by Radovicich and Moissis [15] and Griffith and Snyder [16], the transition from bubbly flow to slug flow in a tube occurs mainly due to agglomerations and coalescences of smaller bubbles into cap bubbles. Once a cap bubble is formed, further coalescences follow in the wake region of a cap bubble. This transition occurs at the void fraction around 0.3. Radovicich and Moissis [15] showed qualitatively that the probability of collisions becomes very large at approximately 0.3, and they postulated this as a cause of the flow-regime transition. Dukler and Taitel [10] proposed 0.3 as the criterion and then used a relative velocity correlation to convert it into a conventional form based on the superficial velocities of liquid and gas. Thus, following these observations, the criterion for the bubbly-to-slug flow transition can be given by

$$\alpha = 0.3. \tag{1}$$

The value of 0.3 can also be obtained from a very simple geometrical consideration only. Suppose bubbles distribute themselves in a tetrahedral lattice pattern in which each bubble fluctuates. It is assumed that there is a sphere of influence around each bubble. Although these spheres of influence can overlap in certain situations, the summation of the sphere volumes equals the total volume of the mixture. The number of not only the collisions but also the coalescences is considered to become very large if the maximum possible gap l between two bubbles becomes less than a bubble diameter $2r_b$ as shown in Fig. 1.

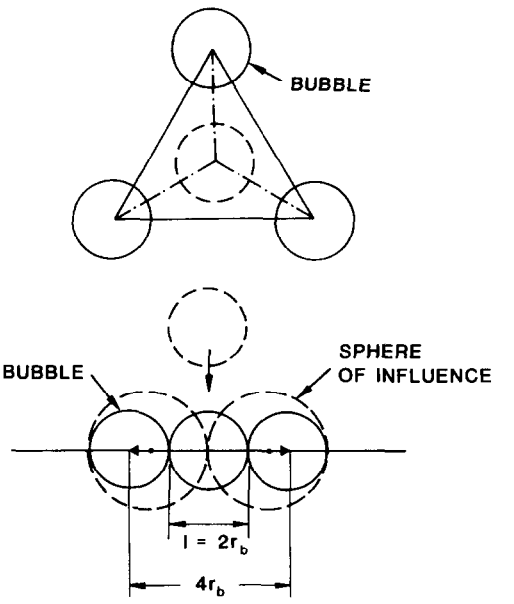

FIG. 1. Bubble packing and coalescence pattern.

Under this condition, it is evident that the bubbles should deform considerably during each fluctuation. The above condition requires that

$$\alpha = \left(\frac{2}{3}\right)^3 = 0.296 \simeq 0.3. \tag{2}$$

In order to convert equation (1) into a conventional form based on the superficial velocities, we use the following relationship between j_g and j_f, which is derived from the drift velocity for bubbly flow [14]

$$\frac{j_g}{\alpha} = C_0 j + \sqrt{2}\left(\frac{\sigma g \Delta\rho}{\rho_f^2}\right)^{1/4}(1-\alpha)^{1.75}, \tag{3}$$

where C_0 is given by

$$C_0 = 1.2 - 0.2\sqrt{\left(\frac{\rho_g}{\rho_f}\right)} \quad \text{for round tubes,} \tag{4}$$

$$= 1.35 - 0.35\sqrt{\left(\frac{\rho_g}{\rho_f}\right)} \quad \text{for rectangular ducts,} \tag{5}$$

and

$$j = j_g + j_f. \tag{6}$$

Therefore, the relationship between j_g and j_f at the transition becomes

$$j_f = \left(\frac{3.33}{C_0} - 1\right) j_g - \frac{0.76}{C_0}\left(\frac{\sigma g \Delta\rho}{\rho_f^2}\right)^{1/4}. \tag{7}$$

2.2. *Slug flow to churn flow transition*

The transition is postulated to occur when the mean void fraction over the entire region exceeds that over the slug-bubble section. This criterion can be visualized in an idealized pattern as follows. At just before the slug-to-churn flow transition, the slug bubbles are lined up right next to each other and the tail of the preceding bubble starts to touch the nose of the following bubble. Under this condition, the liquid slugs become unstable to sustain its individual identity due to the strong wake effect. Then destructions and creations of liquid slug follows. It is considered that physically this corresponds to the flow-regime transition. The mean void fraction over the slug-bubble section α_m is obtained by a potential flow analysis applied to the film flow along the bubble until the film flow reaches the void fraction corresponding to the fully developed flow.

Consider the slug flow model as shown in Fig. 2. Except very near the nose of the bubble, the application of the Bernoulli equation yields the local void fraction at the distance h from the nose, thus

$$\alpha(h) = \frac{\sqrt{(2gh\Delta\rho/\rho_f)}}{\sqrt{(2gh\Delta\rho/\rho_f)} + (C_0 - 1)j + 0.35\sqrt{(\Delta\rho g D/\rho_f)}}, \tag{8}$$

where the following equation for the slug-bubble velocity is used [14]

$$v_{gs} = C_0 j + 0.35\sqrt{\left(\frac{\Delta\rho g D}{\rho_f}\right)}. \tag{9}$$

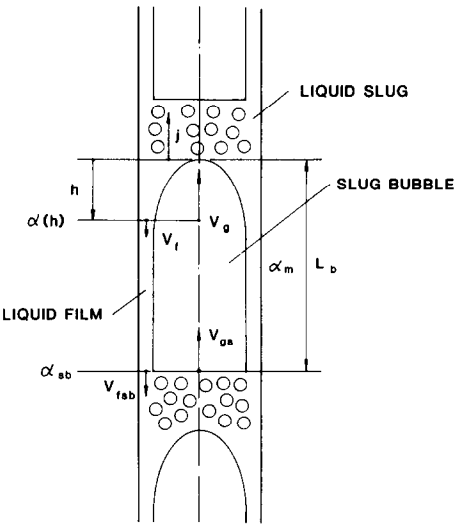

FIG. 2. Slug flow model.

The mean void fraction is calculated by

$$\alpha_m = \frac{1}{L_b}\int_0^{L_b} \alpha(h)\,dh, \tag{10}$$

where L_b is the mean slug-bubble length. Integrating equation (8) and from equation (10), the following equation is derived

$$\alpha_m = 1 - 2X + 2X^2 \ln\left(1 + \frac{1}{X}\right), \tag{11}$$

where

$$X \equiv \sqrt{\left(\frac{\rho_f}{2g\Delta\rho L_b}\right)}\left[(C_0 - 1)j + 0.35\sqrt{\left(\frac{\Delta\rho g D}{\rho_f}\right)}\right]. \tag{12}$$

Equation (11) is well approximated over the numerical values of α_m from 0.6 to 0.9 by the following expression

$$\alpha_m = 1 - 0.813X^{0.75}. \tag{13}$$

Now the mean slug-bubble length L_b at the transition from the slug-to-churn flow regime may be estimated as follows. Somewhere below the nose of a slug bubble, the gravity force on the liquid film is completely balanced by the wall shear stress and the flow becomes fully developed. At a section below this point, there exists a small adverse pressure gradient for the downward liquid film flow. Since the liquids are no longer accelerating in the downward direction, the liquid film becomes unstable due to a flow separation and film instability. Thus, beyond the terminal velocity point of a film, interface disturbances will lead to a cut-off of the slug bubble. The force balance on the liquid film around the slug bubble gives

$$\frac{f}{2}\rho_f v_{fsb}^2 \pi D = \frac{2}{3}\Delta\rho g A(1 - \alpha_{sb}), \tag{14}$$

The factor 2/3 appears on the RHS of the above equation due to the effect of gravity on the wall shear

[13, 14]. The wall friction factor f is assumed to be in the form

$$f = C_f\left[\frac{(1-\alpha_{sb})v_{fsb}D}{\nu_f}\right]^{-m}. \quad (15)$$

Substituting equation (15) into equation (14) and solving for v_{fsb}, we obtain

$$v_{fsb} = (1-\alpha_{sb})^{(1+m)/(2-m)} \times\left[3C_f\left(\frac{D}{\nu_f}\right)^{-m}\frac{\rho_f}{\Delta\rho gD}\right]^{1/(m-2)}. \quad (16)$$

The above equation can be transformed by using the basic relationships for the two-phase mixture, i.e. equation (9) and the following equation

$$v_{fsb} = \frac{\alpha_{sb}v_{gs}-j}{1-\alpha_{sb}}. \quad (17)$$

The resulting equation is

$$\alpha_{sb} = \frac{j+(1-\alpha_{sb})^{3/(2-m)}[3C_f(D/\nu_f)^{-m}(\rho_f/\Delta\rho gD)]^{1/(m-2)}}{C_0 j+0.35\sqrt{(\Delta\rho gD/\rho_f)}}. \quad (18)$$

Here we assume that $m = 0.2$ and $C_f = 0.046$ for a turbulent flow. In the presence of small bubbles in the liquid film section and due to its relatively large film thickness, the film behavior may be approximated by a turbulent flow model for most of the practical cases. Then equation (18) becomes

$$\alpha_{sb} = \frac{j+3ab(1-\alpha_{sb})^{1.67}}{C_0 j+0.35b}, \quad (19)$$

where

$$a \equiv \left(\frac{\Delta\rho gD^3}{\rho_f\nu_f^2}\right)^{1/18}, \quad (20)$$

and

$$b \equiv \sqrt{\left(\frac{\Delta\rho gD}{\rho_f}\right)}. \quad (21)$$

Equation (19) can be solved if we use the approximation

$$(1-\alpha_{sb})^{1.67} \simeq 0.25(1-\alpha_{sb}). \quad (22)$$

Hence we obtain

$$\alpha_{sb} = \frac{j+0.75ab}{C_0 j+0.35b+0.75ab}. \quad (23)$$

On the other hand, equation (8) gives

$$\alpha(L_b) = \frac{y}{y+(C_0-1)j+0.35b}, \quad (24)$$

where

$$y \equiv \sqrt{\left(\frac{2\Delta\rho gL_b}{\rho_f}\right)}. \quad (25)$$

Based on the condition that $\alpha(L_b) = \alpha_{sb}$ at the tail end of the slug bubble, we obtain

$$y = j+0.75ab, \quad (26)$$

or in a more explicit form, the solution for the slug-bubble length becomes

$$\sqrt{\left(\frac{2\Delta\rho gL_b}{\rho_f}\right)} = j+0.75\sqrt{\left(\frac{\Delta\rho gD}{\rho_f}\right)}\left(\frac{\Delta\rho gD^3}{\rho_f\nu_f^2}\right)^{1/18}. \quad (27)$$

There exist several data on the slug-bubble length [5, 17]. Although the general trends are the same among those data, the exact mean bubble lengths are different by as much as 100%. This indicates that the length depends on the development of the slug flow (injection, entry length, etc.). However, when this fact is recognized, Fig. 3 shows a reasonable comparison between Akagawa's data and L_b predicted by equation (27).

Since it is assumed that the transition from the slug-to-churn flow regime occurs when the mean void fraction over the entire region reaches the mean void fraction in the slug-bubble section, the transition criterion becomes

$$\alpha \geqslant 1-0.813 \times\left\{\frac{(C_0-1)j+0.35\sqrt{(\Delta\rho gD/\rho_f)}}{j+0.75\sqrt{(\Delta\rho gD/\rho_f)}(\Delta\rho gD^3/\rho_f\nu_f^2)^{1/18}}\right\}^{0.75}. \quad (28)$$

It is noted that for standard conditions, the term involving 1/18 power in the denominator in the above criterion may be further simplified. For weakly viscous fluids such as water this term may be simply replaced by a constant value of 3, i.e. $(\Delta\rho gD^3/\rho_f\nu_f^2)^{1/18} \simeq 3$. The above criterion is obtained from $\alpha \geqslant \alpha_m$ where α_m is calculated from equation (13) together with equations (12) and (27).

In order to compare equation (28) to existing data in

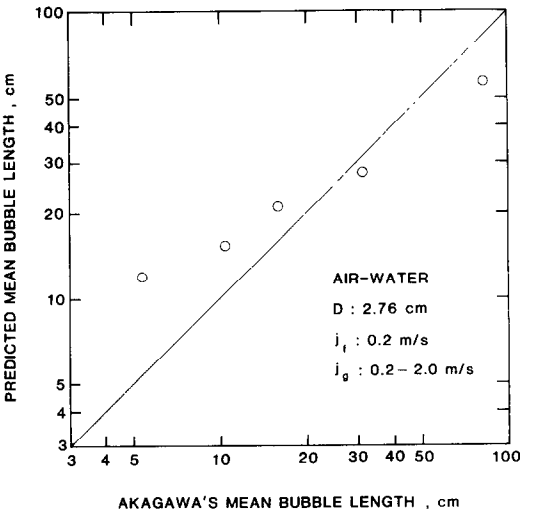

FIG. 3. Comparison of mean bubble length to the experimental data by Akagawa *et al.* [17].

the $j_f - j_g$ plane, the following relationship from the drift-flux model [14] is used

$$\alpha = \frac{j_g}{C_0 j + 0.35(\Delta\rho g D/\rho_f)}. \quad (29)$$

By using equation (29), the transition criterion can be recasted in terms of j_g and j_f under steady-state fully developed flow conditions.

2.3. *Churn flow to annular flow transition*

The criteria for this transition have been developed previously [14], postulating two different mechanisms:

(a) flow reversal in the liquid film section along large bubbles,
(b) destruction of liquid slugs or large waves by entrainment or deformation.

The first mechanism assumes that, for the film section along large bubbles, the annular drift-velocity correlation can be used locally. This can be given by [14]

$$\frac{j_g}{\alpha} - j = \frac{1-\alpha}{\alpha + \{[(1+75(1-\alpha))/\sqrt{\alpha}](\rho_g/\rho_f)\}^{1/2}} \times \left\{ j + \sqrt{\left[\frac{\Delta\rho g D(1-\alpha)}{0.015\rho_f}\right]} \right\}, \quad (30)$$

which can be obtained from a force balance. Hence by setting the flow reversal condition in the film as $j_f = 0$

$$j_g = \sqrt{\left(\frac{\Delta\rho g D}{\rho_g}\right)} \alpha^{1.25} \left\{ \frac{1-\alpha}{0.015[1+75(1-\alpha)]} \right\}^{1/2}. \quad (31)$$

However, in the range of α relevant to the present case, the churn-to-annular flow transition criterion can be approximated by [14]

$$j_g = \sqrt{\left(\frac{\Delta\rho g D}{\rho_g}\right)} (\alpha - 0.11), \quad (32)$$

where α should satisfy the condition given by equation (28).

On the other hand, the second criterion can be obtained from the onset of droplet entrainment [14]. The onset of entrainment criteria for film flow has been developed from a force balance on the liquid wave crest between the shearing force of the vapor drag and the retaining force of the surface tension. This is given by

$$\frac{\mu_f j_g}{\sigma} \sqrt{\left(\frac{\rho_g}{\rho_f}\right)} = N_{\mu f}^{0.8}, \quad (33)$$

where

$$N_{\mu f} \equiv \mu_f \Big/ \left[\rho_f \sigma \sqrt{\left(\frac{\sigma}{g\Delta\rho}\right)}\right]^{1/2}, \quad (34)$$

for low viscous fluid ($N_{\mu f} < 1/15$) and at relatively high liquid Reynolds number ($Re_f > 1635$). It is considered that once the gas flux exceeds the value given above in the churn flow bubble section, the liquid waves and subsequently liquid bridges and slugs can be entrained as small droplets. This will lead to the elimination of liquid slugs between large bubbles and to a continuous gas core. This entrainment induced flow transition is given by the second criterion based on equation (33) as

$$j_g \geq \left(\frac{\sigma g \Delta\rho}{\rho_g^2}\right)^{1/4} N_{\mu f}^{-0.2}. \quad (35)$$

The second criterion is applicable to a flow in a larger diameter tube given by

$$D > \frac{\sqrt{(\sigma/\Delta\rho g)} N_{\mu f}^{-0.4}}{[(1-0.11C_0)/C_0]^2}, \quad (36)$$

Therefore, the second criterion from the onset of entrainment is applicable to predict the occurrence of the annular-mist flow or to predict the churn-to-annular flow transition in a large diameter tube.

Equation (35) can be compared to existing data if we use equation (30) when $\alpha < \alpha_m$, and

$$\alpha = \frac{j_g}{C_0 j + \sqrt{2(\sigma g \Delta\rho/\rho_f^2)^{1/4}}} \quad (37)$$

when $\alpha \geq \alpha_m$.

2.4. *Flow-regime map*

A flow-regime map can be drawn by using newly developed transition criteria. Figure 4 shows an example of a flow-regime map for air–water flow in a 25.4 mm I.D. tube at 25°C and atmospheric pressure.

Curve A on the map designates the bubbly-to-slug flow transition which is predicted by equation (1). The locus of the curve depends only on the properties of both phases. The transition from the slug-to-churn flow occurs at curve B, based on equation (28). At high liquid and gas velocities, the slug flow is limited by curve D corresponding to equation (35). At higher gas velocities than curve D, liquid slugs will be disintegrated into liquid drops by entrainment, thus the annular-mist flow will be observed. However, in Region A, the void fraction is rather low, ranging from 0.3 to 0.7. Thus in this region the flow is so highly agitated that it may be difficult to distinguish between the slug or annular flow. Hence the flow may behave like a churn flow, although it appears to be paradoxical in terms of the standard behavior and definition of the churn flow. The churn-to-annular flow transition occurs at curve C predicted by equation (32). Curve C moves toward higher gas velocities when the tube diameter becomes larger, until the diameter reaches the value which satisfies inequality (36). Therefore, the annular flow which is seen in the region bounded by curves B–D disappears when the diameter is larger than the limiting value.

3. COMPARISON WITH EXISTING DATA

The newly developed flow-regime criteria can be compared with existing data for air–water flow [1, 2, 4–7, 11, 12, 18] and steam–water flow [19–21] under steady-state and fully developed flow conditions, although the present criteria are not limited to these conditions.

In most cases, rather wide discrepancies will be

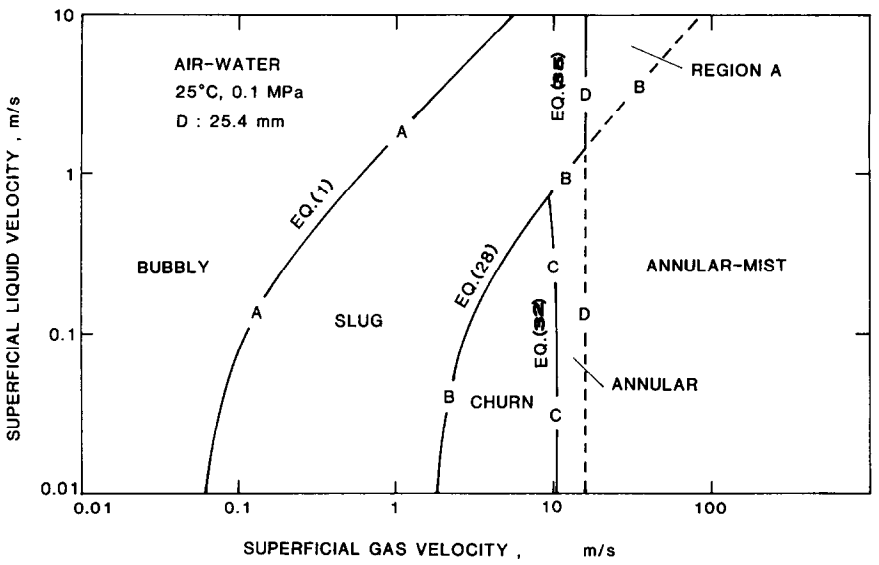

FIG. 4. Flow-regime map based on newly developed transition criteria.

observed in the location of the curves for experimental transition boundaries. This is due to the different methods of observations and definitions of the flow regimes. Moreover, the transition phenomena themselves develop gradually and there are some history effects of upstream conditions. Consequently, some ambiguity is inevitable in determining the transitions. Therefore, the transition boundaries should be understood as a band with a certain width proportional to the uncertainty in determining the transition boundaries.

3.1. *Air–water flow at atmospheric pressure*

Figure 5 shows the comparison of the bubbly-to-slug flow transition for air–water flow at 25°C and atmospheric pressure in a 2.5 cm I.D. tube. Although there are wide discrepancies in the location of the curves, the present criterion predicts intermediate location of the transition boundary. The discrepancy will be attributed mainly to the definition of the bubbly flow, that is, whether the bubbly flow includes cap bubbles or not. For example, the curve by Duns and Ros [6] corresponds to the boundary between Regions I and II, following their terminology. According to their definition, Region I includes part of slug flow as defined by Govier and Aziz [2]. This may be the reason why the curve by Duns and Ros is located at a relatively high gas velocity. Taking into account these facts, the comparison shown in Fig. 5 seems reasonable.

Figure 6 shows the boundaries for the slug-to-churn flow transition for air–water flow at 25°C and atmospheric pressure in a 2.5 cm I.D. tube. The agree-

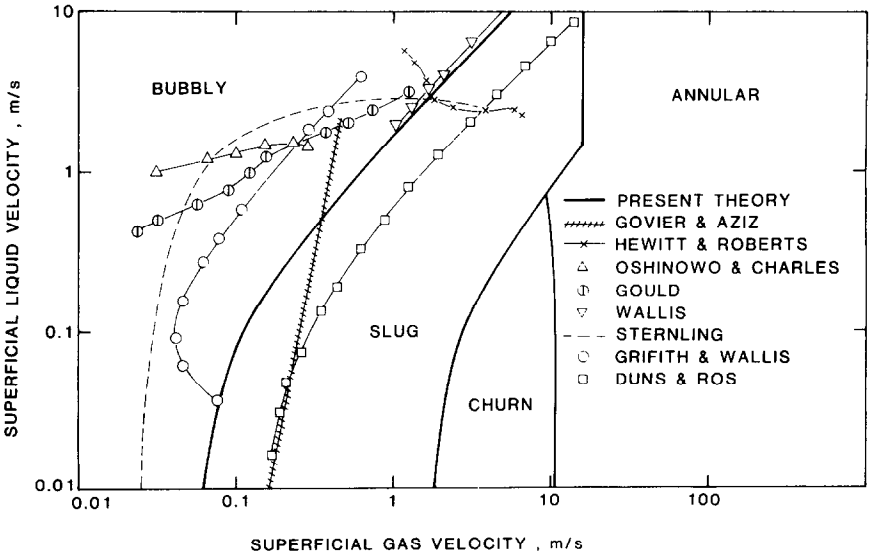

FIG. 5. Comparison of the bubbly-to-slug flow transition for atmospheric air–water flow.

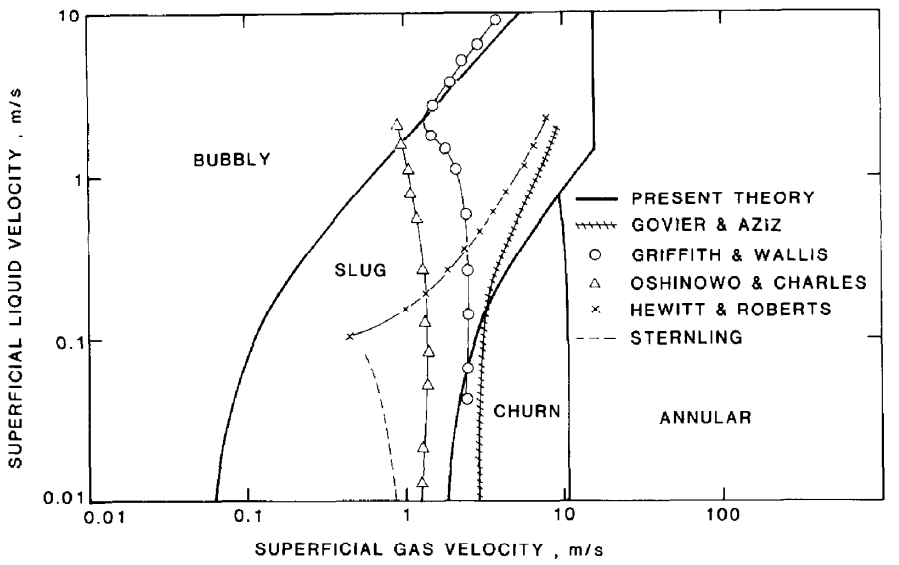

FIG. 6. Comparison of the slug-to-churn flow transition for atmospheric air–water flow.

ment between the present theory and the curve by Govier and Aziz [2] is good and the general trends of the curves which appear in the figure is well reproduced by the theory, except that some of the curves tend to depart from the others at high liquid superficial velocity. This discrepancy may be attributed to the difficulty in discriminating between the churn and slug flow at higher liquid velocities.

The curves for the churn-to-annular flow transition are shown in Fig. 7. A remarkably good agreement is observed in the figure.

Figure 8 compares the present theory with the flow-regime map by Govier and Aziz [2]. Overall agreement is reasonable. Figure 9 shows a good agreement between the present criteria and those of Dukler and Taitel [11]. This agreement is not surprising because the basic principles involved in defining the transition criteria are similar. Figure 10 shows the comparison between the present theory and that of Taitel *et al.* [12]. In the bubbly flow region, they proposed the transition B above which finely dispersed bubbles exist, which the present theory does not distinguish. Transitions A and C may correspond to the curve for the bubbly-to-slug flow transition by the present theory, although Taitel *et al.* [12] postulated the void fraction at the transition to be 0.25 for transition A and 0.52 for transition C instead of 0.3 in the present theory. There is a large disagreement in the boundary between the slug and churn flow at higher liquid volumetric fluxes. This may be attributed to the difference in the proposed basic mechanism of the slug-to-churn flow transition. That is, Taitel *et al.* characterized the churn flow as an entry

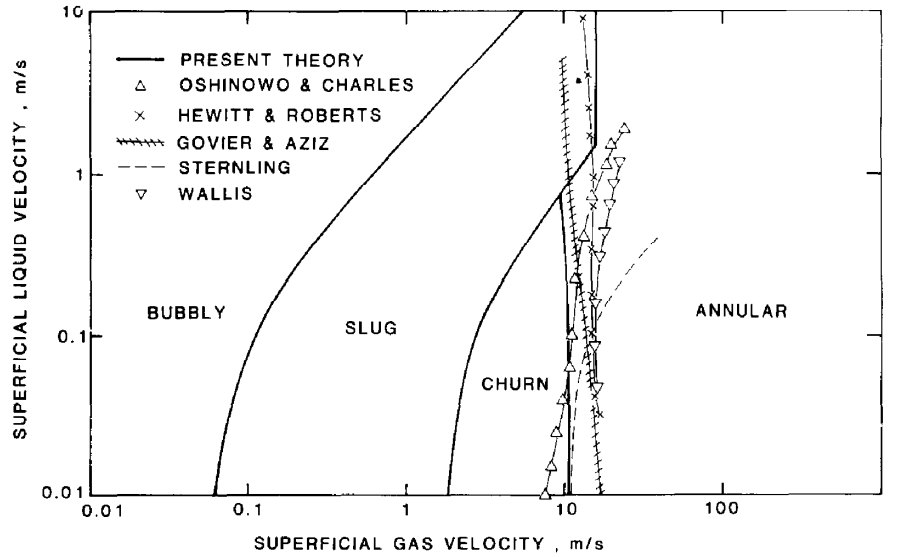

FIG. 7. Comparison of the churn-to-annular flow transition for atmospheric air water flow.

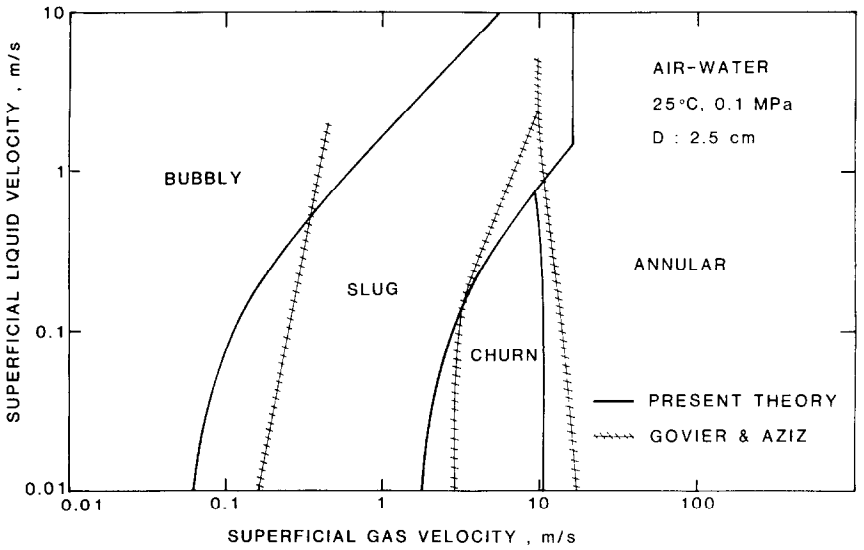

FIG. 8. Comparison to the map of Govier and Aziz [2].

region phenomenon associated with the existence of slug flow further along the pipe, whereas the present theory characterizes it as highly agitated Taylor bubbles and aerated liquid slugs at an increased void fraction. In addition to this, it is very difficult to visually discriminate between these flow regimes at higher liquid velocities, as pointed out by Taitel *et al.* [12]. Finally, transition E corresponds to the boundary of annular flow which agrees very well with the present criterion.

3.2. *Steam–water flow at high pressures*

As most of the maps for vapor–liquid flow are drawn as a relationship between the mass velocity G and the equilibrium vapor quality x_e, the theoretical maps in the j_g–j_f plane are transformed into those in the x_e–G plane. In those cases, the equilibrium vapor quality and the mass velocity are calculated by the following equations

$$G = \rho_g j_g + \rho_f j_f, \tag{38}$$

and

$$x_e = \frac{\rho_g j_g}{G}. \tag{39}$$

The present theory is compared to the data of Bergles *et al.* [19] and Bennet *et al.* [20] for steam–water flow at high pressures in round tubes. Typical comparisons are

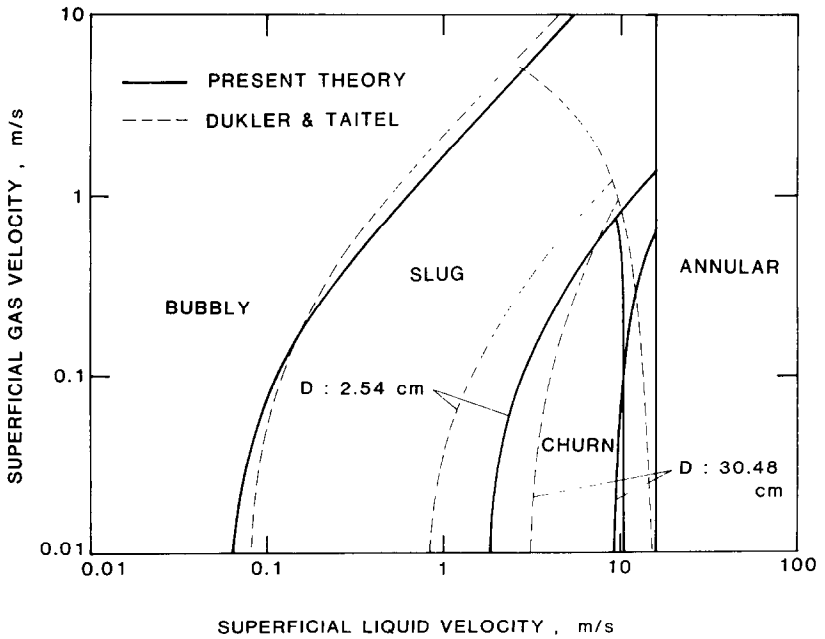

FIG. 9. Comparison to the map of Dukler and Taitel [10]. Air–water at 0.1 MPa.

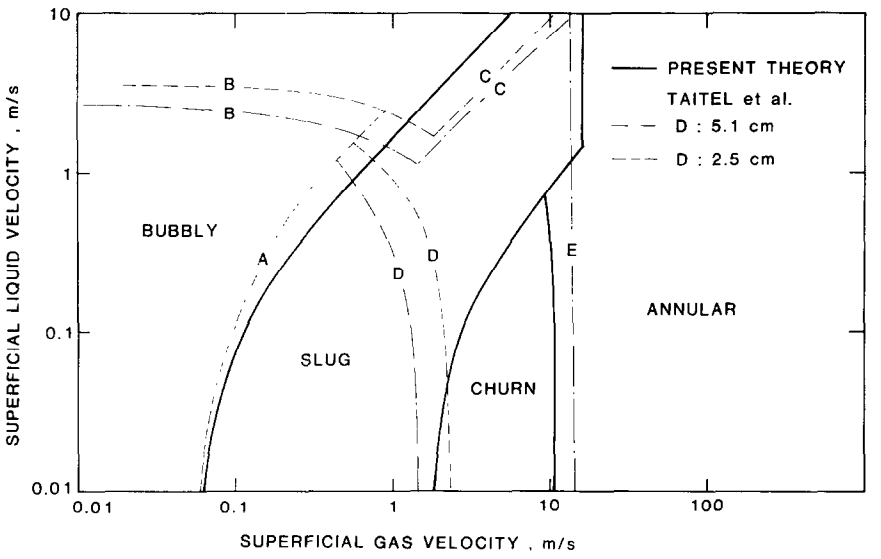

FIG. 10. Comparison to the map of Taitel *et al.* [12]. Water at 0.1 MPa and 25°C.

shown in Figs. 11 and 12. The data were reproduced from ref. [19] in Fig. 11 together with the present flow maps in terms of the mass velocity and the exit vapor quality. The figure demonstrates fairly good agreement between the data and the present criteria. At high mass velocities, the froth flow was observed by Bergles *et al.* [19]. This flow regime appears in the part of the annular flow region where the void fraction is rather low ($0.3 < \alpha < 0.7$) according to our calculation. Hence region A on the present flow map, where the flow may behave like a highly agitated churn flow, may correspond to the froth flow regime.

The maps can also be plotted in terms of the superficial velocities of both phases as shown in Fig. 13. As the experimental data are originally plotted in terms of the mass velocity vs equilibrium vapor quality, the superficial velocities for the data points are calculated from those parameters by assuming thermal equilibrium. However, provided that the subcooling is not very large, the calculated superficial velocities will be good estimates of the true values. It is interesting to note, by comparing Fig. 12 with, say, Fig. 8, that the locus of the curve for the bubbly-to-slug flow transition is almost unchanged, whereas the locus of the curve for the churn-to-annular flow transition moves toward lower gas velocities at higher pressures.

An example of the map affected by subcooled boiling is shown in Fig. 14. The broken lines represent the

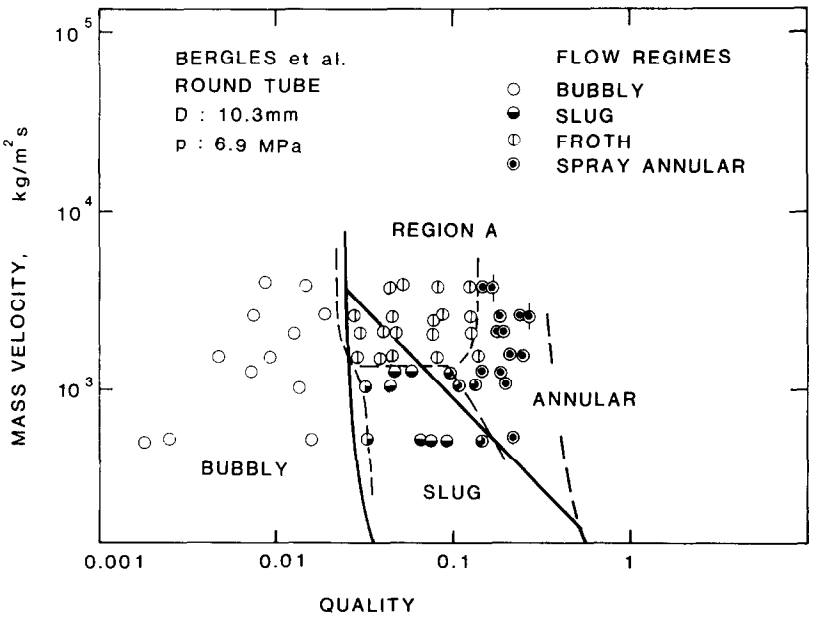

FIG. 11. Flow-regime map for steam–water flow at 6.9 MPa in a 10.3 mm I.D. tube, compared to the data of Bergles *et al.* [19]. Water at 0.1 MPa and 25°C.

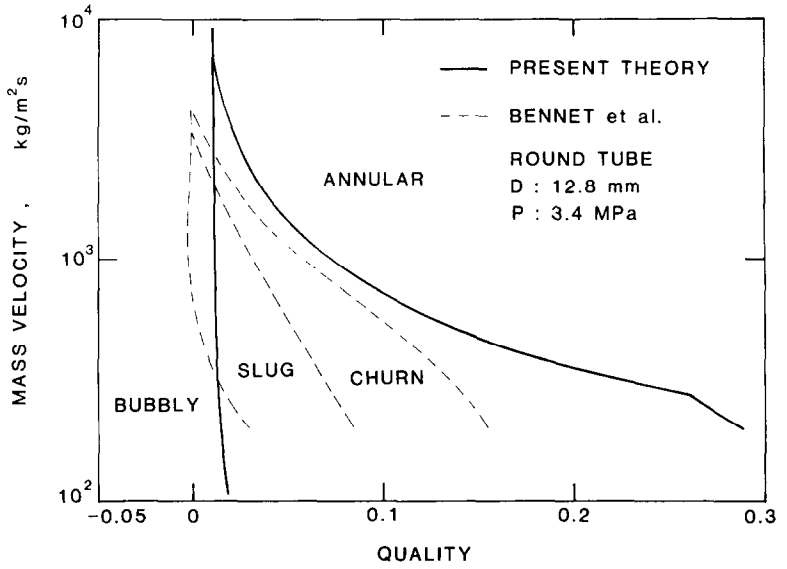

FIG. 12. Semi-logarithmic flow-regime map compared to the data of Bennet *et al.* [20] for subcooled flow boiling at 3.4 MPa.

transition boundaries reproduced from the data of Bergles *et al.* [19] for 3.4 MPa steam–water flow in a 29.9 mm I.D. tube. The curves turn away from the theoretical map as the mass velocity is increased.

Figure 14 shows that the use of thermal equilibrium quality may not be accurate for the flow-regime map when subcooled boiling occurs at higher mass velocities. In the present theory, the criteria for the flow-regime transition are correlated in terms of the void fraction and the volumetric fluxes. In view of this, flowing quality will be more relevant to use in plotting the experimental data in the flow map [21] for non-equilibrium flow. The data in Fig. 14 can be transformed to the one shown by the broken lines in which the flowing quality was estimated by using the Levy correlation [22] together with the Bowring correlation [23] for the subcooling at the point of bubble detachment. The dotted solid-line represents the bubbly-to-slug flow transition based on the thermal equilibrium quality. The figure shows the relevance of the use of the flowing quality in non-equilibrium (subcooled boiling) flow.

The comparison of the theory with the data for high pressure steam–water flow in a rectangular channel is

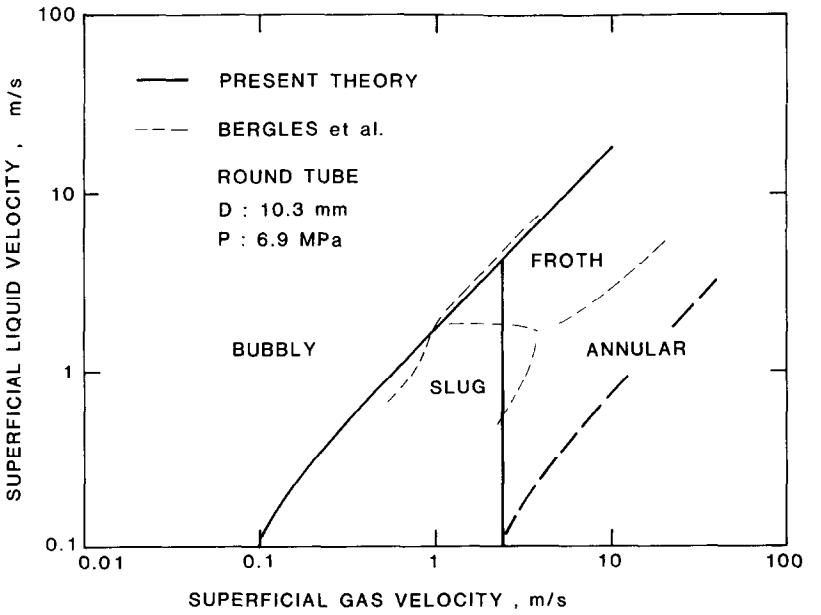

FIG. 13. Comparison of the flow-regime map in terms of the superficial velocities for steam–water flow at 6.9 MPa in a 10.3 mm I.D. tube.

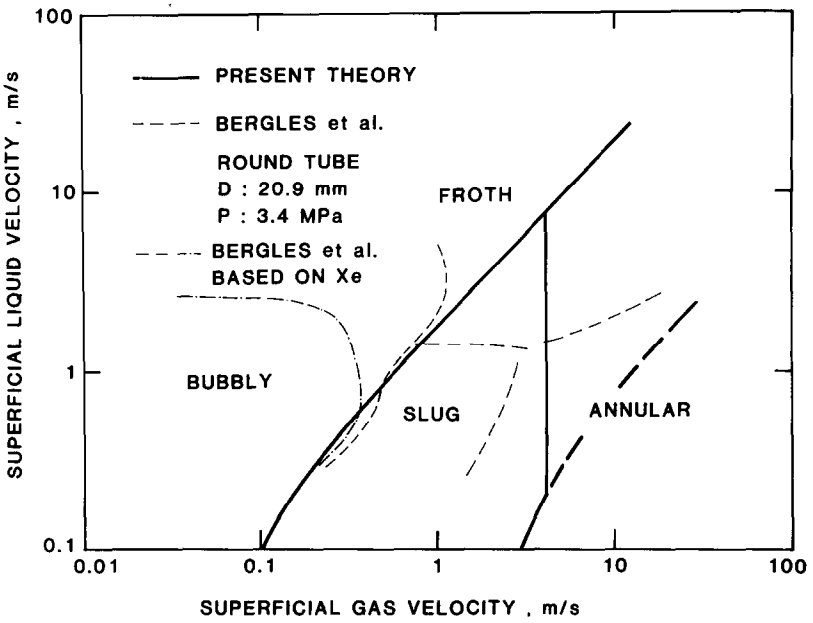

FIG. 14. Comparison of the flow-regime map in terms of the superficial velocities for steam–water flow at 3.4 MPa in a 20.9 mm I.D. tube.

presented in Figs. 15–19. The data were reproduced from ref. [24]. In these figures, the data are plotted in terms of mass velocity vs flowing quality. Hosler used flowing quality instead of thermal equilibrium quality in order to account for subcooled boiling and for some of the effects of heat flux, as mentioned by himself [24]. Figures 15–19 indicate that the general trends are very similar to those for steam–water flows in round tubes and are predicted reasonably well by the present theory, except that the agreement of the bubbly-to-slug flow transition is disappointing at 1.0 MPa. However, Hosler himself limited the applicable range of pressure to 2–14 MPa for use of his data with reasonable confidence.

The theory can be compared to those data in terms of the volumetric fluxes, too. The example is presented in Fig. 20. The theoretical flow-regime maps indicate that the slug-to-annular flow transition occurs at lower gas velocities with increasing pressure, although the trend is less remarkable in the experimental data.

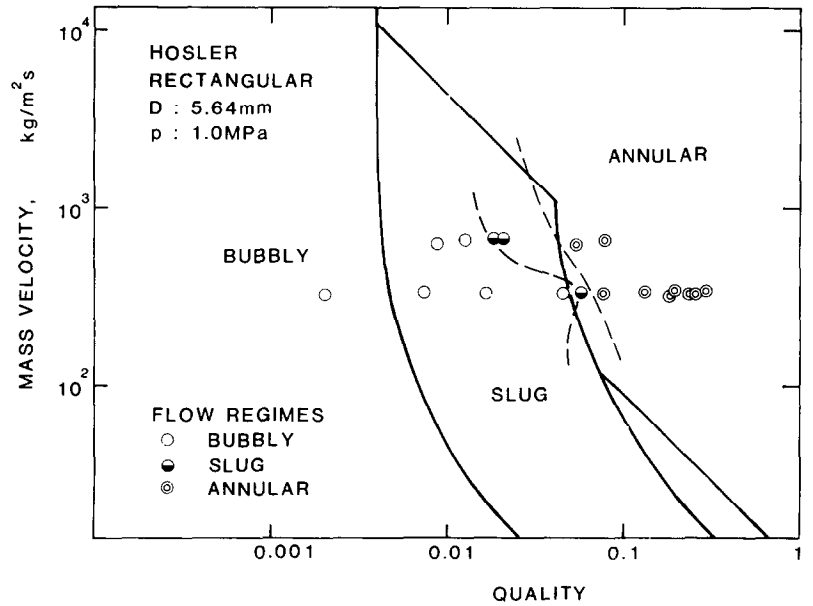

FIG. 15. Comparison for steam–water flow at 1.0 MPa in a rectangular channel (data taken by Hosler [24]).

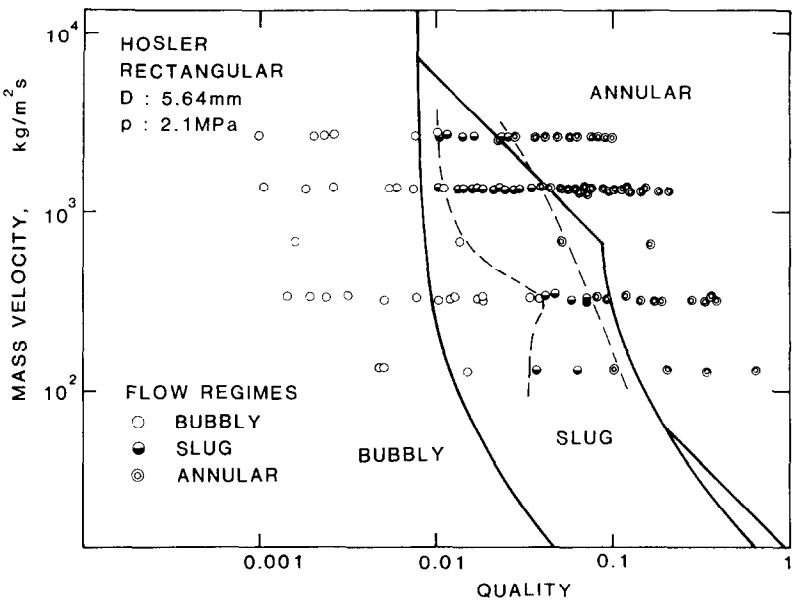

FIG. 16. Comparison for steam–water flow at 2.1 MPa in a rectangular channel (data taken by Hosler [24]).

4. SUMMARY AND CONCLUSIONS

Traditional flow-regime criteria based on the gas and liquid superficial velocities are not suitable to the two-fluid model formulation. For a two-fluid model, direct geometrical parameters such as the void fraction should be used in flow-regime criteria. From this point of view, new flow-regime criteria have been developed for a vertical upward flow. These new criteria can be compared to existing data under steady-state and fully developed flow conditions by using relative velocity correlations obtained previously [14].

Newly developed criteria have been compared with the conventional criteria and experimental data for atmospheric pressure air–water flows and high pressure steam–water flows in round tubes and a rectangular channel. There exist wide discrepancies among the experimental data, not only due to the different methods of observations and definitions of the flow regimes but also due to the transition phenomena themselves which develop gradually. However, when these factors are considered, it could be said that the present criteria showed satisfactory agreements with those data.

It is also pointed out that the flowing quality is more suitable than the thermal equilibrium quality to

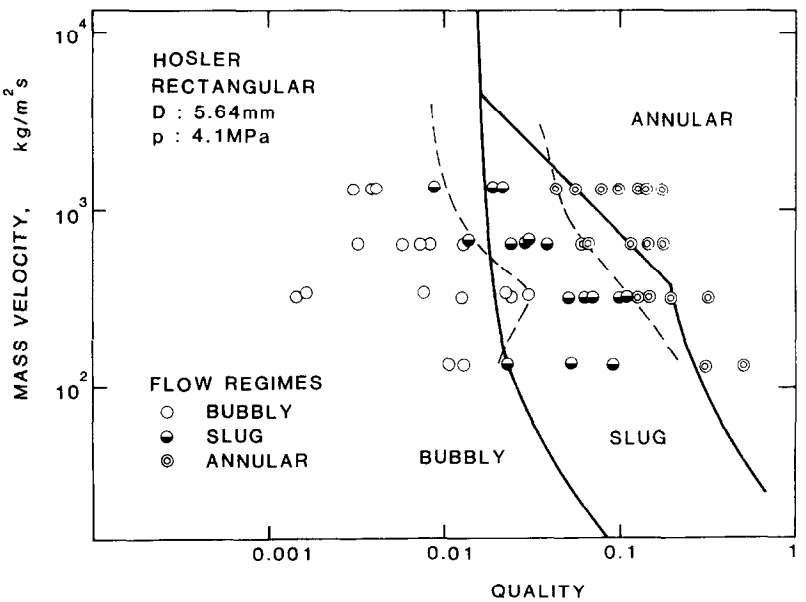

FIG. 17. Comparison for steam–water flow at 4.1 MPa in a rectangular channel (data taken by Hosler [24]).

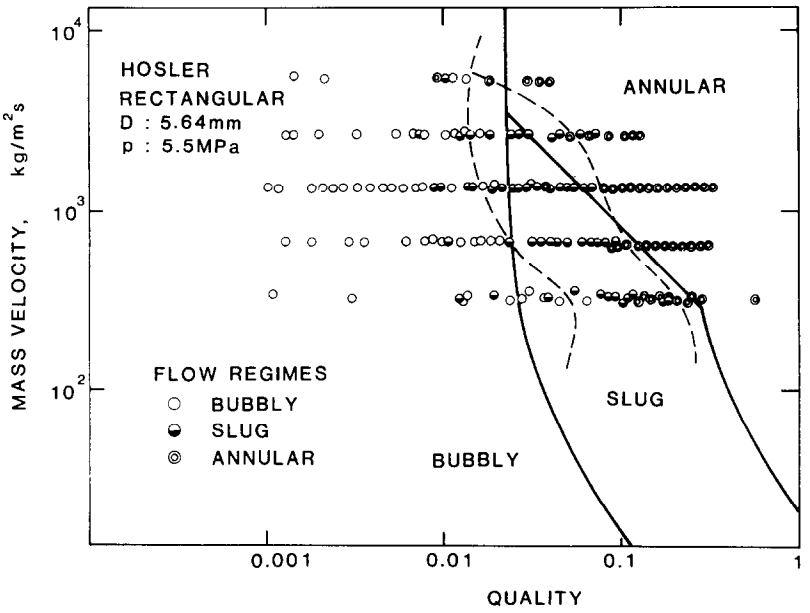

FIG. 18. Comparison for steam–water flow at 5.5 MPa in a rectangular channel (data taken by Hosler [24]).

correlate the flow-regime transitions for a subcooled-boiling system. This is consistent with the statement that the void fraction should be used in flow-regime criteria.

Acknowledgements—Part of this work was performed under the auspices of the U.S. Nuclear Regulatory Commission.

REFERENCES

1. V. C. Sternling, Two phase flow theory and engineering decision, award lecture presented at AIChE Annual Meeting, December (1965).
2. G. W. Govier and K. Aziz, *The Flow of Complex Mixtures in Pipes*. Van Nostrand Reinhold, New York (1972).
3. G. B. Wallis, *One-dimensional Two-phase Flow*. McGraw-Hill, New York (1972).
4. G. F. Hewitt and D. N. Roberts, Studies of two-phase flow patterns by simultaneous X-ray and flash photography, UKAEA Report AERE-M2159 (1969).
5. P. Griffith and G. B. Wallis, Two-phase slug flow, *J. Heat Transfer* **83C**(3), 307 (1961).
6. H. Duns, Jr. and N. C. J. Ros, Vertical flow of gas and liquid mixtures from borcholes, *Proc. 6th World Petroleum Congress*, Frankfurt, June (1963).
7. T. L. Gould, Vertical two-phase steam–water flow in geothermal wells, *J. Petroleum Technol.* **26**, 833 (1974).

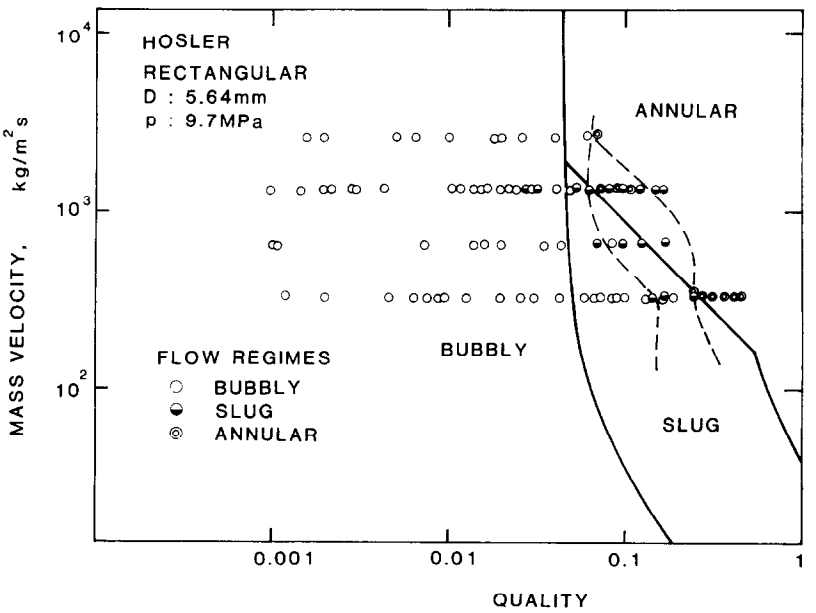

FIG. 19. Comparison for steam–water flow at 9.7 MPa in a rectangular channel (data taken by Hosler [24]).

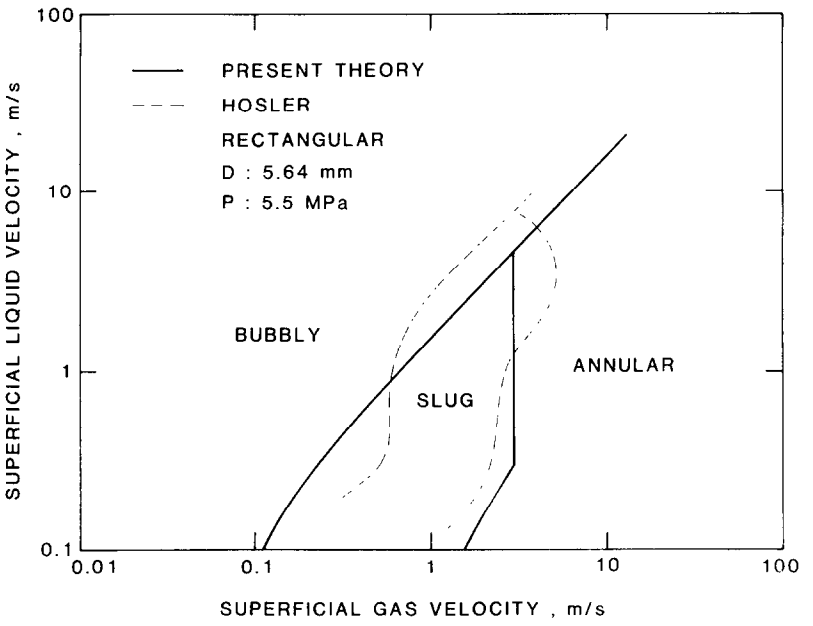

FIG. 20. Flow-regime map in terms of the superficial velocities for Hosler's data at 5.5 MPa.

8. P. L. Spedding and V. T. Nguyen, Regime maps for air water two phase flow, *Chem. Engng Sci.* **35,** 779 (1980).
9. J. Weisman and S. Y. Kang, Flow pattern transitions in vertical and upwardly inclined lines, *Int. J. Multiphase Flow* **7,** 271 (1981).
10. A. E. Dukler and Y. Taitel, Flow regime transitions for vertical upward gas liquid flow: a preliminary approach through physical modeling, Progress Report No. 1, NUREG-0162 (1977).
11. A. E. Dukler and Y. Taitel, Flow regime transitions for vertical upward gas liquid flow, Progress Report No. 2, NUREG-0163 (1977).
12. Y. Taitel, D. Bornea and A. E. Dukler, Modelling flow pattern transitions for steady upward gas–liquid flow in vertical tubes, *A.I.Ch.E. Jl* **26**(3), 345 (1980).
13. G. F. Hewitt and N. S. Hall-Taylor, *Annular Two-phase Flow*. Pergamon Press, Oxford (1970).
14. M. Ishii, One-dimensional drift-flux model and constitutive equations for relative motion between phases in various two-phase flow regimes, ANL Report ANL-77-47 (1977).
15. N. A. Radovicich and R. Moissis, The transition from two-phase bubble flow to slug flow, MIT Report No. 7-7633-22 (1962).
16. P. Griffith and G. A. Snyder, The bubbly–slug transition in a high velocity two-phase flow, MIT Report No. 5003-29 (1964).
17. K. Akagawa, H. Hamaguchi and T. Sakaguchi, Studies on the fluctuation of pressure drops in two-phase slug flow (Third Report, Pressure recovery behind a bubble, and bubble and liquid slug lengths), *Trans. Japan Soc. Mech. Engng* **36**(289), 1535 (1970).
18. T. Oshinowo and M. E. Charles, Vertical two-phase flow: Part II. Holdup and pressure drop, *Can. J. Chem. Engng* **56,** 438 (1974).
19. A. E. Bergles, J. P. Roos and J. G. Bourne, Investigation of boiling flow regimes and critical heat flux, NYO-3304-13 (1968).
20. A. W. Bennet, G. F. Hewitt, H. A. Kearsey, R. K. F. Keeys and P. M. C. Lacey, Flow visualization studies of boiling at high pressure, UKAEA Report AERE-R4874 (1965).
21. K. Sekoguchi, O. Tanaka, S. Esaki, N. Katsuki and M. Nakasatomi, Prediction method of flow patterns in subcooled and low quality boiling regions, *Trans. Japan Soc. Mech. Engrs* **46**(409), 1825 (1980) in Japanese.
22. S. Levy, Forced convection subcooled boiling—prediction of vapor volumetric fraction, *Int. J. Heat Mass Transfer* **10,** 951 (1967).
23. R. W. Bowring, Physical model based on bubble detachment and calculations of steam voidage in the subcooled region of a heated channel. Report HPR-10, OECD Halden Report Project (1962).
24. E. R. Hosler, Flow patterns in high pressure two-phase (steam–water) flow with heat addition, *Chem. Engng Prog. Symp. Ser.* **64**(82), 54 (1968).

CRITERES DE REGIME D'ECOULEMENT TRANSITOIRE POUR UN ECOULEMENT DIPHASIQUE ASCENDANT DANS DES TUBES VERTICAUX

Résumé—Les critères classiques de régime d'écoulement diphasique basés sur les vitesses surfaciques de gaz et de liquides ne peuvent être convenables pour les analyses des écoulements d'entrée ou rapidement variables par le modèle à deux fluides. Dans ces conditions, on postule que les paramètres géométriques directs tels que la fraction de vide sont plus simples et plus utilisables dans les critères de régime d'écoulement que les paramètres adimensionnels. De ce point de vue, des nouveaux critères de régime d'écoulement pour l'ascension dans des tubes verticaux ont été développés en considérant les mécanismes de transition de régime d'écoulement. Ces nouveaux critères peuvent être comparés aux critères existants et aux données expérimentales de régime permanent et d'écoulement pleinement établi en utilisant des corrélations de vitesses relatives. Les critères montrent des accords raisonnables avec les données relatives aux écoulements eau–air atmosphérique. D'autres comparaisons ont été faites avec des données pour eau–vapeur d'eau dans les tubes circulaires et un canal rectangulaire à des pressions relativement élevées. Les résultats confirment que les critères présentés ici peuvent être appliqués dans un large domaine de paramètres aussi bien qu'à l'écoulement en ébullition.

ÜBERGANGSKRITERIEN BEIM STRÖMUNGSVERHALTEN FÜR AUFWÄRTS GERICHTETE ZWEIPHASENSTRÖMUNGEN IN SENKRECHTEN ROHREN

Zusammenfassung—Die traditionellen Kriterien für das Verhalten von Zweiphasenströmungen, die auf den Geschwindigkeiten an den Oberflächen basieren, eignen sich nicht zur Untersuchung von schnell veränderlichen oder Eintrittsströmungen mit Hilfe des Zwei-Fluid-Modells. Unter diesen Umständen wird postuliert, daß direkte geometrische Parameter wie Porosität begrifflich einfacher und deshalb verläßlicher im Gebrauch im Zusammenhang mit Kriterien des Strömungsverhaltens sind als die herkömmlichen Parameter. Von diesem Gesichtspunkt ausgehend, wurden neue Kriterien für aufwärts gerichtete Gas–Flüssigkeits-Strömungen in senkrechten Rohren entwickelt, die die Mechanismen der Änderungen des Strömungsverhaltens berücksichtigen. Diese neuen Kriterien können mit bestehenden Kriterien und Versuchsdaten im Fall der stationären und vollausgebildeten Strömung verglichen werden, indem Beziehungen mit der Relativgeschwindigkeit angewendet werden. Die Kriterien zeigten gute Übereinstimmungen mit vorhandenen Daten für atmosphärische Luft–Wasser-Strömungen. Darüber hinaus werden Vergleiche mit Daten für Dampf–Wasser in runden Rohren und einem Rechteckkanal bei relativ hohen Systemdrücken durchgeführt. Die Ergebnisse bekräftigen, daß die gegenwärtigen Kriterien für die Änderungen des Strömungsverhaltens sowohl über weite Bereiche der Parameter als auch beim Strömungssieden angewendet werden können.

КРИТЕРИИ ПЕРЕХОДА РЕЖИМОВ ТЕЧЕНИЯ ДВУХФАЗНЫХ ВОСХОДЯЩИХ ПОТОКОВ В ВЕРТИКАЛЬНЫХ ТРУБАХ

Аннотация—Традиционно используемые критерии двухфазного режима течения, определяемые из скоростей фильтрации газа и жидкости, могут оказаться непригодными для анализа высокоскоростного неустановившегося потока или потока на входе с помощью двухжидкостной модели. В этих условиях предполагается, что такие непосредственно определяемые геометрические параметры, как объемная доля пустот, являются более простыми, а поэтому более надежными для использования в качестве критериев режима течения. Исходя из этого, на основе рассмотрения механизмов перехода режимов течения предложены новые критерии для восходящих газожидкостных потоков в вертикальных трубах. Их можно сравнить с имеющимися критериями и экспериментальными данными для стационарных и полностью развитых течений, используя соотношения для относительных скоростей. Критерии хорошо согласуются с имеющимися экспериментальными данными для атмосферных течений воздуха и воды. Кроме того, проведены сравнения с данными по течению воды и пара в круглых трубах и прямоугольном канале при относительно высоких давлениях в системе. На основе анализа результатов установлено, что предлагаемые критерии перехода режимов течения (в том числе для течений с кипением) могут использоваться в широких диапазонах изменения параметров.